

Force and Bias Dependent Contrast in Atomic Force Microscopy Based Photocurrent Imaging on GaAs-AIAs Heterostructures

W. Brezna, G. Strasser, J. Smoliner

Institut für Festkörperelektronik, TU Wien,
Floragasse 7, A-1040 Wien, Austria

In this work, photocurrent images of lithographically processed GaAs/AIAs heterostructures are recorded by an atomic force microscope. It is found that the AFM tip-sample contact is strongly dependent on the thickness of the native oxide layer on the sample surface. Therefore the photocurrents increase if a successively increasing tip-sample force is applied, which leads to a gradual penetration of the surface oxide layer. Due to the complex behavior of the photocurrent as a function of tip-bias and tip-force, the contrast in photocurrent images is non-monotonic and can be reversed under appropriate bias and force conditions.

Introduction

Photocurrent spectroscopy is a very versatile tool to investigate a wide range of effects in solids. The fact that electric currents can easily be measured down to the fA regime and the possibility to use very high power light sources to excite the sample leads to an exceptional high sensitivity. Due to this high sensitivity, one can even gain information about optically “forbidden” transitions [1] – [3]. Photocurrent spectroscopy applications range from investigations of interband [3], intraband, intersubband [4], [5] and intrasubband [6] transitions in heterostructures and quantum dot systems [7] – [9] to investigations of organic films [10], organic devices [11] and the analysis of dielectric materials [12]. Some efforts have been made to increase the spatial resolution of photocurrent measurements by either using shadow masks to define the illuminated sample areas [13] or by using a carefully focused and collimated beam of light [14]. One can also find some scanning near field optical microscopy (SNOM) approaches to increase the spatial resolution into the nm-regime [15].

For the characterization of materials in the nanometer regime, Scanning Probe Microscopy (SPM) based methods are the prime choice beside Scanning Electron Microscopy and Transmission Electron Microscopy. Spatially resolved optical absorption measurements have already been performed with a scanning tunneling microscope (STM) to investigate the influence of the laser irradiation on the differential conductance on an InAs covered GaAs sample surface [16]. Other groups were using the STM tip as a local Schottky contact to perform photocurrent measurements [17]. Only recently conductive Atomic Force Microscopy (cAFM) was applied to study InAs wires on GaAs [18]. However, these investigations were all performed either at low temperatures and / or under high vacuum conditions. Although this is leading to much more idealized experimental conditions, the experiments are much more demanding and time consuming.

In this work we present Atomic Force Microscopy (AFM) based photocurrent imaging experiments, which were performed under ambient conditions. We want to investigate

the details of the photocurrent contrast generation on a lithographically patterned GaAs-AlAs reference sample, e.g. how the locally collected photocurrent depends on the applied tip sample voltage and tip sample contact force beside the obvious local variations of the sample. For the AFM based photocurrent experiments the AFM feedback laser was chosen as a light source and the photocurrent is collected locally via the electrically conducting tip of an AFM.

Experimental

Figure 1 shows the assumed band profile of the AFM-tip–sample system used for photocurrent imaging under zero bias. The sample has a photodiode design as it is frequently used for the investigation of InAs quantum dots [19]. The sample consists of n⁺-GaAs followed by an intrinsic layer of GaAs for charge separation. On top of the intrinsic region a 10 nm AlAs barrier layer was grown and a cap layer of 10 nm GaAs was introduced to avoid oxidation. For plotting the band diagram in Fig. 1, we assumed the Fermi level at the GaAs surface to be pinned at a position near midgap about 0.6 eV to 0.8 eV lower than the conduction band edge of GaAs [20], [21].

Standard photolithography was used to remove the GaAs cap layer and the AlAs barrier on one part of the sample to define sample regions with properties. The sample structuring was done by applying selective etch solutions to remove the GaAs cap layer selective to AlAs (citric acid : H₂O₂ = 2.4 mol/l : 1 mol/l for 20s). In a second etching step, the AlAs was removed selectively to GaAs using 0.02 mol/l NaOH for 9 minutes.

To guarantee good electrical contact, InSn pellets were diffused into the sample surface at 450 °C for 5 minutes. Conductive silver was used to contact the InSn pellets on the sample surface and to glue the sample on a gold covered nickel sample plate. A gold wire was then used between the sample plate and the magnetic plate holder of the AFM to ensure a reliable electrical contact.

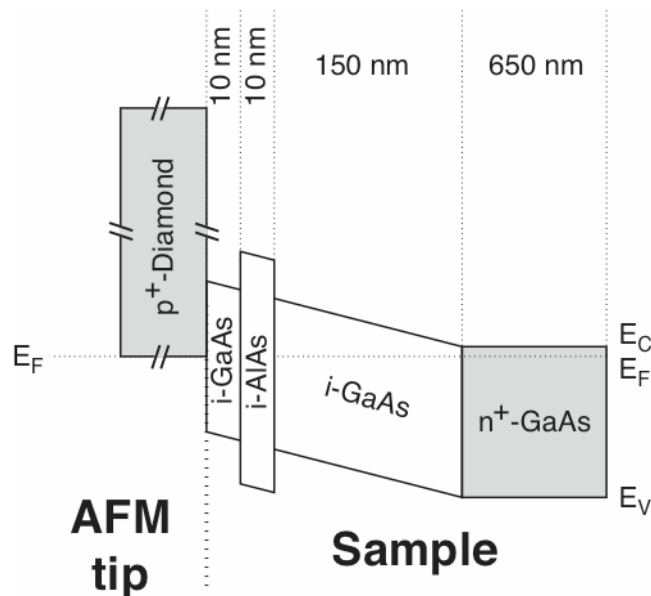


Fig. 1: Band profile of the AFM-tip–sample system under zero bias condition and ideal AFM-tip–sample contact (layer thickness not to scale). The intrinsic substrate is omitted. E_F is the Fermi level, E_C and E_V mark the conduction and valence band edges.

The AFM used in this work was a Molecular Imaging, PicoPlus system with closed loop scanner and PicoScan 3000 controller. The photocurrent measurements were performed using the built-in current-voltage preamplifier with an amplification of 10^8 V/A. The preamplifier was located in direct vicinity to the tip to minimize parasitic wire capacitance and to ensure the bandwidth of approximately 300 Hz in the fA – nA regime required for photocurrent imaging applications. As AFM tips we used highly doped (p-type 1×10^{20} cm⁻³) conductive diamond tips (NanoWorld) which show superior resistance against abrasion. The tips' high spring constant of 40 N/m (as it is normally used for scanning spreading resistance measurements) ensures a good electrical contact to the sample, but care must be taken not to scratch the sample surface by using too high forces. As light source, the AFM feedback laser (1mW @ 670nm) was used in the present experiments. The laser diameter was approximately 60 μ m leading to a nominal laser intensity of 28 W/cm². Note that the actual laser intensity hitting the investigated sample spot will be lower, due to shadowing effects caused by the AFM tip.

Measurements

Figure 2(a) shows a topographic AFM image of the sample after removing the AIAs barrier on one part of the sample by using photolithography. The non-etched area is labeled A and the area where the 10 nm GaAs cap-layer and the 10 nm AIAs barrier were removed is labeled with B. The measured edge height was 24 nm, which agrees quite well with the nominal 20 nm thickness of these layers.

Figure 2(b) shows two current vs. voltage (IV) curves recorded on areas A and B without any incident light (complete darkness). During the measurement, the AFM camera illumination as well as the AFM feedback laser was switched off and the AFM system was shielded from ambient light. The sweep duration for a single IV curve was only 5s, therefore the frozen AFM feedback during that time led to no issues concerning tip drifts or changes in contact force. Due to the AIAs barrier present in area A, the forward current onset occurs at higher bias values than in area B. In the reverse biased range between 0 V and -2 V no significant dark current could be detected both in area A as well as in area B.

Figure 2(c) shows typical IV spectra recorded under illumination. Under illumination, a distinct photocurrent under reverse bias is observed in areas A and B. The voltage dependence of the photocurrent, however, differs significantly in both areas.

The photocurrent in area B first shows a strong increase with reverse bias. At higher reverse voltages, however, the photocurrent saturates. This behavior can be attributed to the fact that ideally, the photocurrent is only limited by the carrier generation rate, which is proportional to the incident light power. In contrast to that, however, the reverse current in area A shows an *exponential* increase with the reverse voltage. In addition, the current in area A is lower than in area B at low applied reverse bias values, which is most likely due to the influence of the AIAs blocking layer. At higher reverse voltage, however, the current in area A even exceeds the current in area B although the power of the incident light is the same. A possible explanation for this astonishing fact can be found in a publication by Capasso *et al.* [22], who showed that the electron impact ionization and the corresponding carrier multiplication factor in a AlGaAs/GaAs heterostructure is strongly enhanced. If we also assume an enhancement of avalanche carrier generation in area A, this would explain both that the current in area A exceeds the saturation current in area B (due to avalanche generation) and the exponential current characteristics in A (due to the exponential increase of the multiplication factor with voltage).

The photocurrent vs. voltage measurements were also performed for 3 different tip-sample forces (0.17 μ N, 0.5 μ N and 3.3 μ N). As one can see in Figure 2(c), an in-

crease in force leads to an increase of the photocurrent in both areas A and B. It must be pointed out that the increase of force has a much larger effect on the photocurrent in area A than in area B. Obviously, this behavior must be related to the presence of the AIAs layer in this area.

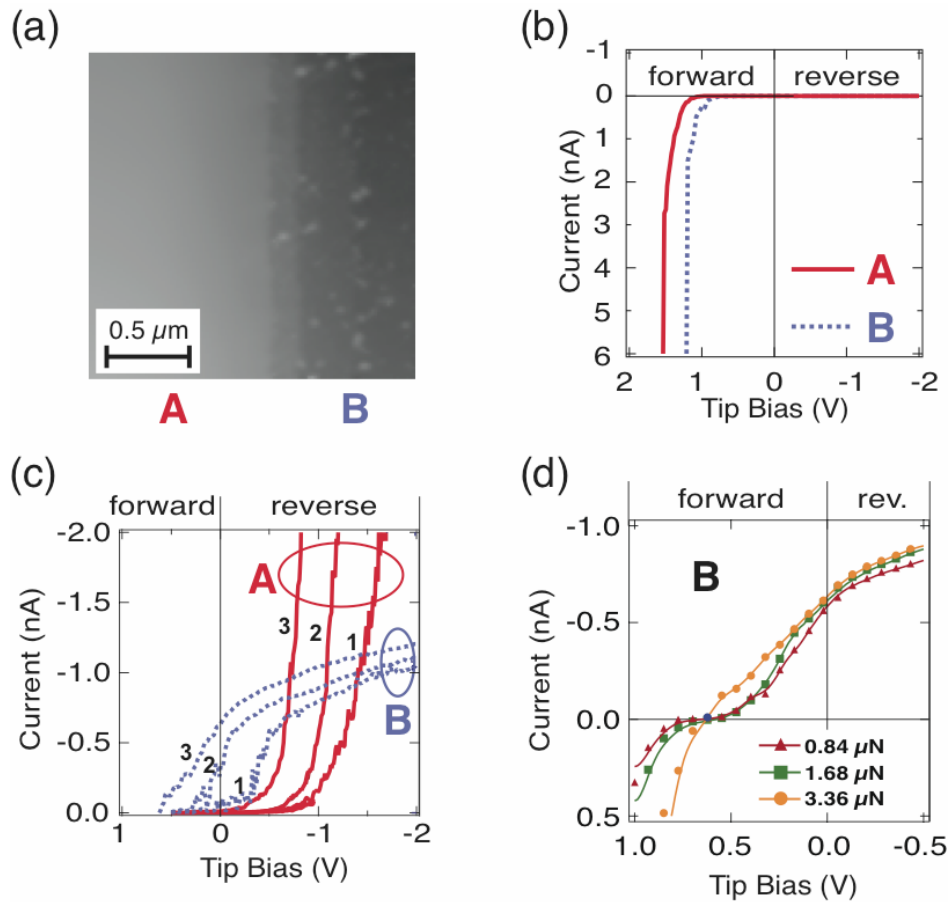


Fig. 2: (a) Topographic AFM image of the sample after etching away the AIAs barrier and GaAs cap layer on part B of the sample. (b) I-V characteristics of area A (straight line) and area B (dotted line) without illumination at tip sample force of $0.17 \mu\text{N}$. (c) I-V characteristics of area A (straight lines) and area B (dotted lines) under illumination ($1\text{mW @ } 670\text{nm}$) and at different applied tip sample forces (curves (1): $0.17 \mu\text{N}$, (2): $0.5 \mu\text{N}$ and (3): $3.3 \mu\text{N}$). (d) I-V characteristic of area B under illumination at different applied tip forces for different voltage and current ranges.

As an explanation for the tip force dependence of the IV curves, we assume the existence of a layer of native oxide on the sample surface. Under the ambient conditions where the measurements were performed, all samples are usually covered with such a thin layer of native oxide. Even after the routinely applied HCl dips to remove the oxide layer from the GaAs sample, only a few minutes under ambient air conditions again lead to the formation of a significant amount of native oxide on the sample surface. This oxide layer acts as an additional barrier for the photo generated carriers, which can be overcome by applying higher negative tip bias values. Another possibility to overcome the barrier is to successively penetrate the native oxide by increasing the tip force, which successively decreases the thickness of the oxide barrier. The consequences of this procedure are illustrated in Fig. 2(c), where a set of force dependent IV-curves are shown.

At a low force of $0.17 \mu\text{N}$ (figure 2 (c), curve 1, area B) a significant photocurrent only occurs below -0.3 V . At higher forces of $0.5 \mu\text{N}$ (curve 2) and $3.3 \mu\text{N}$ (curve 3), the onset of the photocurrent in area B is shifted to the left by the reduced oxide barrier thickness. In contrast to that, the voltage required for zero current flow (the open circuit voltage V_{oc}) does *not* change with increasing force. This can be seen in Fig. 2(d), where the force dependent IV curves clearly intersect at the same tip voltage position of $V_{\text{tip}} = V_{\text{oc}} = +0.62 \text{ V}$ for all tip forces in the shown range.

The oxide layer does also influence the electrical behavior above V_{oc} (forward biased region). Here the oxide layer acts as an additional energetic barrier in series to the Schottky barrier which becomes thinner with increasing tip force. As a consequence, the forward current increases with tip force, and the observed characteristic approaches the well known IV characteristic of solar cells for higher tip forces.

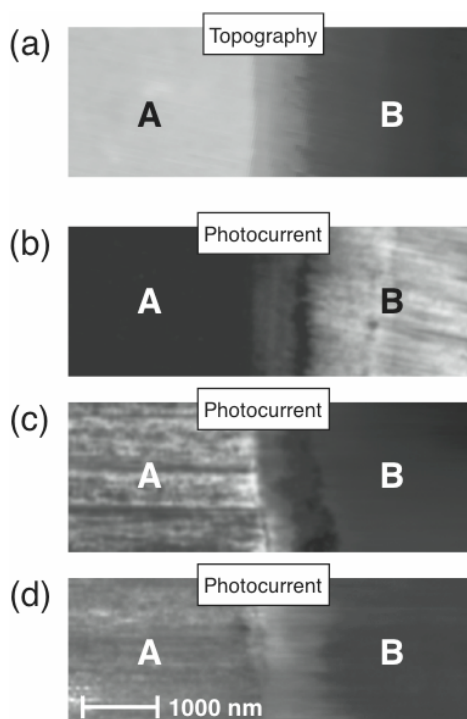


Fig. 3: (a) Topographic AFM image of the sample. (b) – (d): Corresponding photocurrent images recorded for different voltage and force value combinations. (b): low voltage, low force (-0.8 V , $0.17 \mu\text{N}$), (c): high voltage, low force (-1.8 V , $0.17 \mu\text{N}$), (d) low voltage, high force (-0.8 V , $3.3 \mu\text{N}$).

The photocurrent's complex dependence on the applied bias and on the applied tip sample force has a severe impact on the contrast in photocurrent imaging. Figure 3 (a) again shows the topographic AFM image of the etch step on the sample surface together with the simultaneously recorded photocurrent data for different applied bias voltages and tip sample forces (Fig. 3(b) – (d)). As light source for the photocurrent imaging again the AFM feedback laser was used. For a low applied reverse voltage and force (-0.8 V , $0.17 \mu\text{N}$ see Fig. 3(b)) one can see good photocurrent contrast between area A and area B. However, increasing the applied (reverse) bias voltage leads to a complete contrast reversal in Fig. 3(c), where an image recorded at *high* reverse voltage and low force (-1.8 V , $0.17 \mu\text{N}$) is shown. Leaving the applied voltage at low values but increasing the tip sample force also leads to a photocurrent contrast reversal, which can be seen in Fig. 3(d). These imaging results are in good agreement with the discussion of the plot displayed in Fig. 2(c).

Summary

In summary, we have shown that photocurrents measured by AFM techniques are highly dependent on the applied bias voltage and tip sample force. The force dependence of the electrical tip-sample contact was explained by the presence of a native oxide layer on the sample. The AFM tip can successively penetrate this oxide layer with increasing applied tip force which gives rise to an increasing photocurrent. The photocurrent contrast turned out to be non monotonic. Depending on the force and the tip bias, complete contrast reversal can be obtained. Finally, the photocurrent in areas where the AIAs barrier was present showed an exponential increase as a function of reverse bias, which can be related to electron avalanche multiplication in AIAs/GaAs heterostructures. These findings demonstrate the importance of well defined experimental parameters, especially tip-sample force and tip-sample bias, for reproducible photocurrent measurements with an AFM.

Acknowledgements

This work was sponsored by FWF project SFB-025 TP08.

References

- [1] R.T. Collins, L.Viña, W. I. Wang, L.L. Chang, L. Esaki, K.v.Klitzing, K. Ploog, *Phys. Rev. B* 36, Vol. 3, 1531 (1987)
- [2] K. Yamanaka, T. Kukunaga, N. Tsukada, K. L. I. Kobayashi, M. Ishii, *Appl. Phys. Lett.* 48, 840 (1986)
- [3] K. Tanaka, N. Kotera, H. Nakamura, *J. Appl. Phys.* 85 (8), 4071-4075 (1999)
- [4] R. P. Leavitt, J. W. Little, *Appl. Phys. Lett.* 79, 2091 (2001)
- [5] X. L. Huang, Y. G. Shin, E. K. Suh, H. J. Lee, Y. G. Hwang, Q. Huang, *J. Appl. Phys.* 82, 4394 (1997)
- [6] R. J. Stone, J. G. Michels, S. L. Wong, C. T. Foxon, R. J. Nicholas, A. M. Fox, *Appl. Phys. Lett.* 69, 3569 (1996)
- [7] L. Chu, A. Zrenner, G. Böhm, G. Abstreiter, *Appl. Phys. Lett.* 76(14), 1944 (2000)
- [8] S. Sauvage, P. Boucaud, T. Brunhes, V. Immer, E. Finkman, J. M. Gérard, *Appl. Phys. Lett.* 78, 2327 (2001)
- [9] L. Höglund, C. Asplund, Q. Wang, S. Almqvist, H. Malm, E. Petrini, J. Y. Andersson, P. O. Holtz, H. Pettersson, *Appl. Phys. Lett.* 88, 213510 (2006)
- [10] C. L. Yang, Z. K. Tang, W. K. Ge, J. N. Wang, Z. L. Zhang, X. Y. Jian, *Appl. Phys. Lett.* 83(9), 1737 (2003)
- [11] M. Breban, D. B. Romero, S. Mezheny, V. W. Ballarotto, E. D. Williams, *Appl. Phys. Lett.* 87, 203503 (2005)
- [12] V. J. Kapoor, F. J. Feigl, S. R. Butler, *Phys. Rev. Lett.* 39, 1219 (1977)
- [13] G. Fasching, F. F. Schrey, W. Brezna, J. Smoliner, G. Strasser, K. Unterrainer, *Phys. Stat. Sol. C* 2(8), 3114 (2005)
- [14] A. V. Andrianov, S. R. A. Dods, J. Morgan, J. W. Orton, T. M. Benson, I. Harrison, E.C. Larkins, F.X.Daiminger, E.Vassilakis, J.P.Hirtz, *J. Appl. Phys.* 87(7), 3227 (2000)
- [15] A. Richter, J. W. Tomm, Ch. Lienau, J. Luft, *Appl. Phys. Lett.* 69(26), 3981 (1996)

- [16] T. Takahashi, M. Yoshita, I. Kamiya, H. Sakaki; Appl. Phys. A 66, S1055 (1998)
- [17] E. Beham, A. Zrenner, G. Böhm; Physica E 7, 359 (2000)
- [18] H. Masuda, M. Takeuchi, T. Takahashi; Ultramicroscopy 105, 137 (2005)
- [19] M. Kroutvar, Y. Ducommun, J. J. Finley, M. Bichler, G. Abstreiter, A. Zrenner; Appl. Phys. Lett. 83, 443 (2003)
- [20] T. Sugino, T. Itagaki, J. Shirafuji; Diam. Rel. Mat. 5, 714 (1996)
- [21] W.E. Spicer, P.W. Chye, P.R. Skeath, C.Y. Su, I. Lindau; J. Vac. Sci. Technol. 16, 1422 (1979)
- [22] F.Capasso, W.T.Tsang, A.L.Hutchinson, G.F.Williams, Appl. Phys. Lett. 40, 38 (1982)